

A Comparative study on generalized Manev potential and Newtonian potential in perturbed restricted four-body problem

Jagadish Singh¹ Omale Solomon Okpanachi²

Abstract. The motion of a test particle within the context of the restricted four-body problem (R4BP) driven by a new kind of potential, called the generalized Manev potential, with perturbations in the Coriolis and centrifugal forces is considered in this study. The system possesses eight libration points which were distributed on its plane of motion in different manner from those of the usual Newtonian potential. Unlike the case of the perturbed R4BP under Newtonian potential, where two of these librations are stable, all of them are unstable in linear sense under Manev potential. We found that a gradual perturbation in the centrifugal force causes the trajectories of motion to drift inward but the Coriolis force was proven to have no effect on the location of the libration points of the system. Using first order Lyapunov characteristic exponents, the dynamical behavior of the system is found irregular. We experimented with a high velocity stellar system (82 G. Eridani) to establish the applicability of the model in astrophysics.

§1 Introduction

Modified Newtonian potential is the new frontier in the studies of the dynamics of gravitating particle systems. In recent times, researches have shown that there are lapses in using the classical Newton's law of gravitation to explain certain phenomena such as the orbit of the Moon around the Earth and the observed perihelion advances of Mercury in solar dynamics. Following these limitations, Newton in [1] demonstrated that a central-force problem having this kind of potential $\frac{A}{r} + \frac{B}{r^2}$ leads to a precessional elliptic relative orbit. The general relativity theory excelled in explaining well such phenomena in both quantitative and qualitative manner, but according to Diacu [2] formulating relativistic n -body problem is difficult.

However, in Maneff [3],[4],[5],[6] the Bulgarian Physicist George Manev obtained a similar model in the twenties, and proposed a suitable substitute for the relativity theory. Manev came

Received: 2019-11-13. Revised: 2020-06-09.

MR Subject Classification: 00A71, 35A01, 65N12.

Keywords: generalized Manev potential, Coriolis force, centrifugal force, stability, chaotic, 82 G. Eridani.

Digital Object Identifier(DOI): <https://doi.org/10.1007/s11766-023-3964-9>.

up with a potential of form $\frac{\mu}{r} + \frac{3\mu^2}{2C^2r^2}$, where μ is the gravitational parameter of the two-body and C the speed of light. Several authors have investigated the restricted few-body problem with Manev-type forces. For instance, Blaga [7] worked on the precessing orbits, central forces and Manev potential; Ivanov and Prodanov [8] studied Manev potential and general relativity; Haranas and Mico [9] investigated Manev potential and satellite orbits; Kirk et al [10] examined satellite motion in a Manev potential with drag. Blaga [11] considered circular orbits, Lyapunov stability and Manev-type forces. Barrabes et al [12] studied spatial collinear restricted four-body problem with repulsive Manev potential by considering a quasi-homogeneous potential of the form $-(\frac{a}{r} + \frac{e}{r^2})$, where a and e are real constants and r is the distance between the particles.

Various factors such as variation of the mass of the primaries, Coriolis force, PR drag, Stokes drag, oblateness of participating bodies, radiation pressure force and centrifugal force, etc are studied as generalization in the restricted few-body. Several researchers such as Bhatnager and Hallan[13], Singh and Aguda[14], Singh and Omale [15], Singh and Omale [16], Vincent et. al [17], Abouelmagad et al [18] have considered the effects of little perturbations in the Coriolis and centrifugal forces in the framework of restricted few- body problem.

Our motivation in this study is to carry out a numerical investigation of the motion of a test particle in the gravitational field of three primaries having Lagrangian configuration under the effect of small perturbations in the Coriolis and centrifugal forces together with the bodies possessing Manev potential. Also, we carried out a comparative study of the motion of the infinitesimal body in the cases of Newtonian potential and Manev potential. The governing equations of motion for the system are set up in section 2. In sections 3 and 4 the equilibrium points and the linear stability were studied respectively, then section 5 is for the determination of Chaos using LCEs, while section 6 is the model application to a stellar system, namely, 82. G Eridani. Finally, the discussion and conclusion are presented in section 7.

§2 GOVERNING EQUATIONS OF MOTION

We take cue from [12], [13], [14] and [15] to set up the equations of motion for the system. Given that three point-masses m_1 , m_2 and m_3 are in circular motion about their centre of mass which is fixed at the origin of the coordinate system and are at the vertices of an equilateral triangle. A fourth mass m taken as a test particle in motion in the same plane under the influences of the force of gravity of the three bodies and the triangle is oriented in such a manner where m_1 is placed on the positive x-axis and m_2, m_3 having equal masses, are positioned symmetrically with relative to x- axis. Normalizing the unit of the system, let the point masses add up to be 1 and the respective distances between them also equal to 1 and time unit is chosen so that the gravitational constant G and mean motion n are also a unity. Let the coordinates of the test particle be (x, y) and those of the point masses m_1, m_2 and m_3 be $(\sqrt{3}\mu, 0)$, $(-\frac{\sqrt{3}}{2}(1-2\mu), \frac{1}{2})$ and $(-\frac{\sqrt{3}}{2}(1-2\mu), -\frac{1}{2})$ respectively. With $\mu = \frac{m_2}{m_1+m_2+m_3} = \frac{m_3}{m_1+m_2+m_3}$ as the mass parameter. The equations that govern the motion of the test particle under perturbations in the Coriolis (α) and centrifugal forces (β) with the generalized Manev

potential in the rotating frame of reference are given as

$$\left. \begin{aligned} \ddot{x} - 2\alpha\dot{y} &= \frac{\partial\Omega}{\partial x} \\ \ddot{y} + 2\alpha\dot{x} &= \frac{\partial\Omega}{\partial y} \end{aligned} \right\} \quad (2.1)$$

With

$$\Omega = \frac{\beta}{2} (x^2 + y^2) + (1 - 2\mu) \left(\frac{1}{r_1} + \frac{3(1 - 2\mu)}{2c^2 r_1^2} \right) + \mu \left(\frac{1}{r_2} + \frac{3\mu}{2c^2 r_2^2} \right) + \mu \left(\frac{1}{r_3} + \frac{3\mu}{2c^2 r_3^2} \right) \quad (2.2)$$

$$\begin{aligned} r_1^2 &= (x - \sqrt{3}\mu)^2 + y^2 \\ r_2^2 &= \left(x + \frac{1}{2}\sqrt{3}(1 - 2\mu)\right)^2 + \left(y - \frac{1}{2}\right)^2 \\ r_3^2 &= \left(x + \frac{1}{2}\sqrt{3}(1 - 2\mu)\right)^2 + \left(y + \frac{1}{2}\right)^2 \\ r^2 &= x^2 + y^2 \end{aligned}$$

$$\begin{aligned} \alpha &= 1 + \varepsilon, & |\varepsilon| &\ll 1, \\ \beta &= 1 + \varepsilon', & |\varepsilon'| &\ll 1 \end{aligned}$$

where $\varepsilon, \varepsilon'$ represent perturbations in the Coriolis and the centrifugal forces respectively and c is the speed of light. Following the concept of Dubeibe [19], we normalize by setting $c = 1$. More so, to enable our investigations switch between the classical Newtonian potential and the generalized Manev potential, we use the following transformation

$$\frac{1}{c^2} \rightarrow \sigma \frac{1}{c^2}$$

Where σ is the Manev parameter and taking $c = 1$, equation (2.2) becomes

$$\begin{aligned} \Omega &= \frac{\beta}{2} (x^2 + y^2) + (1 - 2\mu) \left(\frac{1}{r_1} + \frac{3\sigma(1 - 2\mu)}{2r_1^2} \right) \\ &+ \mu \left(\frac{1}{r_2} + \frac{3\sigma\mu}{2r_2^2} \right) + \mu \left(\frac{1}{r_3} + \frac{3\sigma\mu}{2r_3^2} \right), \quad \sigma \in [0, 1]. \end{aligned} \quad (2.3)$$

Taking $\sigma = 0$ we realise the classical Newtonian potential, for $\sigma \in (0, 1]$, we have the Manev potential case, while for $\sigma \in [-1, 0)$ we have the repulsive Manev potential case. We shall be using the Potential function in Equation (2.3) all through our computations and investigations.

§3 Location of Libration Points

The points of libration or equilibrium correspond to the positions in the plane where the influence of gravity and the centrifugal force associated with the rotating coordinate system cancel each other, with the implication that a test particle (say an artificial satellite or a circumstellar dust) positioned at one of these libration points appears stationary in the rotating frame. Therefore at the libration points $\ddot{x} = \ddot{y} = \dot{x} = \dot{y} = 0$. It thus follow from Equations (2.1) and (2.3), that the equilibrium points are solutions of

$$\begin{aligned} & \beta x - (1 - 2\mu) \left(x - \sqrt{3}\mu \right) \left(\frac{1}{r_1^3} + \frac{3\sigma(1 - 2\mu)}{r_1^4} \right) \\ & - \mu \left(x + \frac{1}{2}\sqrt{3}(1 - 2\mu) \right) \left(\frac{1}{r_2^3} + \frac{3\sigma\mu}{r_2^4} \right) \\ & - \mu \left(x + \frac{1}{2}\sqrt{3}(1 - 2\mu) \right) \left(\frac{1}{r_3^3} + \frac{3\sigma\mu}{r_3^4} \right) = 0 \end{aligned} \tag{3.1}$$

$$\begin{aligned} \beta y - (1 - 2\mu) y \left(\frac{1}{r_1^3} + \frac{3\sigma(1 - 2\mu)}{r_1^4} \right) - \mu \left(y - \frac{1}{2} \right) \left(\frac{1}{r_2^3} + \frac{3\sigma\mu}{r_2^4} \right) - \mu \left(y + \frac{1}{2} \right) \left(\frac{1}{r_3^3} + \frac{3\sigma\mu}{r_3^4} \right) \\ = 0 \end{aligned} \tag{3.2}$$

It is intuitive to observe that Eqs. (3.1) and (3.2) are independent of α . This shows that Coriolis force perturbation has no effect on the positions of libration points. The solutions of Eqs. (3.1) and (3.2) are points of intersection of the curves in the xy-plane. When $y = 0$, $\sigma = 0.8$, $\mu = 0.0190$, and $\beta = 1$, two collinear points $L_{1,2}$ were obtained on the x-axis and six non-collinear points L_j ($j=3,4,\dots,8$), as shown in figs. 1 and 2 respectively. Similar results are observed in Baltagiannis and Papadakis[20] and [14].

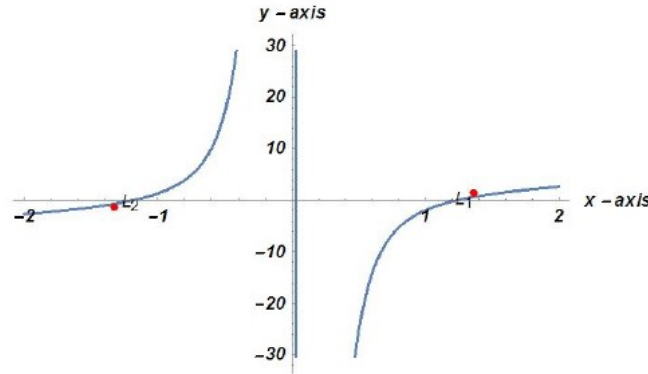


Figure 1. The two collinear points in red colour with the blue lines as the path of motion for the test particle.

Tables 1 and 2 show the results of the equilibrium points for the increasing value of perturbation in the centrifugal force parameter β with fixed Manev parameter $\sigma = 0.8$

We observe from the tables 1 and 2 above that with the increasing value of perturbation in the centrifugal force, there are notable changes in the positions of collinear and non-collinear libration points that result in gradual inward shift of the trajectories of the infinitesimal mass. Fig 1 shows that there is no difference in the number of the collinear libration point even if the equation of motion is governed by Manev potential. Fig 3 reveals this obvious shifting of the trajectories and instead of the usual dumbbell contour around the two equal masses in the case of classical Newtonian potential as shown in Fig 4, the Manev potential gives a highly distorted

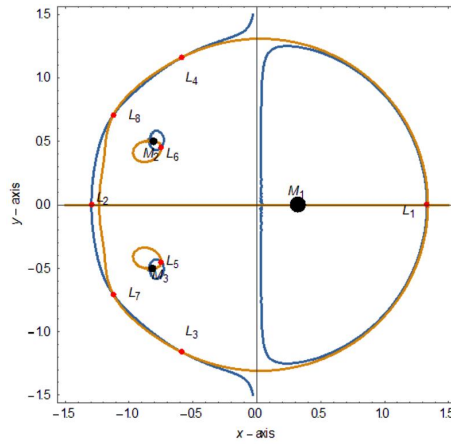


Figure 2. The eight equilibrium points without perturbation; the blue and the yellow lines are the contours of the orbit of the test particles with the red as the point of interception.

Table 1. collinear libration points at constant Manev parameter.

β	L_1	L_2
1.0	1.397620	-1.363740
1.1	1.361960	-1.327310
1.2	1.330280	-1.294880
1.4	1.276080	-1.239270
1.44	1.266440	-1.229350
1.6	1.231070	-1.192950
1.8	1.192800	-1.153460

Table 2. Increasing Centrifugal force and the six non-collinear libration points at constant Manev parameter $\sigma = 0.8$.

β	$L_{3,4}$	$L_{5,6}$	$L_{7,8}$
1.0	-0.624035 1.218980	-0.752644 0.453444	-1.170370 0.747898
1.1	-0.605657 1.187860	-0.751817 0.453012	-1.145790 0.725343
1.2	-0.590338 1.159650	-0.750966 0.452571	-1.124060 0.706105
1.4	-0.566350 1.110230	-0.749191 0.451656	-1.087520 0.675150
1.44	-0.562375 1.101270	-0.748824 0.451468	-1.081150 0.669922
1.6	-0.548558 1.068010	-0.747313 0.450698	-1.058240 0.651545
1.8	-0.534976 1.031250	-0.745324 0.449694	-1.034520 0.633187

irregular contour or orbit as shown in Fig 2.

In Fig 5 we have compared the effect of different potentials with respect to the orbit of the infinitesimal mass. The inner orbit corresponds to the Newtonian potential, while the

outer orbit is for the Manev potential. It shows that the Newtonian potential gives a smaller orbit than the Manev potential. Illustratively, Fig 5 suggests that all things being equal, a space asset undertaking motion on the Newtonian orbit might have an economic advantage in terms of fuel consumption, because the period of the motion will usually be lesser than that of the model designed on the Manev orbit. However, in the case of luminous primaries, the electro-mechanical components of a space asset on the Newtonian orbit might experience high adverse effect than a space asset on a Manev orbit, because the Newtonian (i.e the inner) orbit is closer to the primaries. More so, the positions of libration points for the test particle are not distributed in similar manner under the Manev potential and the Newton potential. This suffices that the objective of a given space mission will determine the kind of potential that is suitable for the model. In the nutshell, the Newtonian potential is an approximation of the Manev potential in both quantitative and qualitative sense.

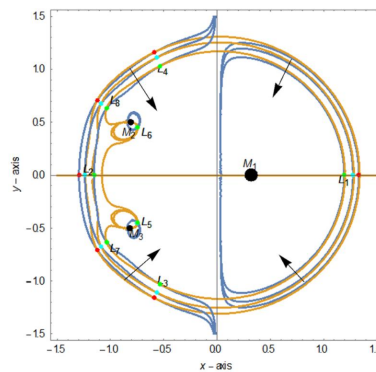


Figure 3. The orbit of the infinitesimal mass shifting inward with increasing centrifugal force under Manev potential. The red point is when $\beta = 1$, the cyan point is when $\beta = 1.4$ and the green point is when $\beta = 1.6$.

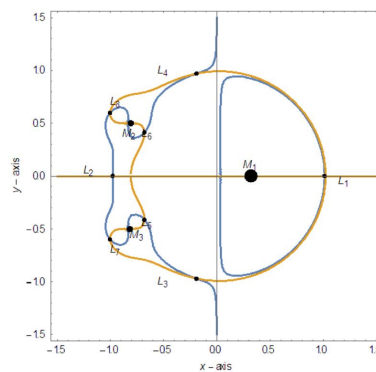


Figure 4. The orbit of the infinitesimal mass under Newtonian Potential with the blue and the yellow lines as the contours and the black points as the equilibrium points.

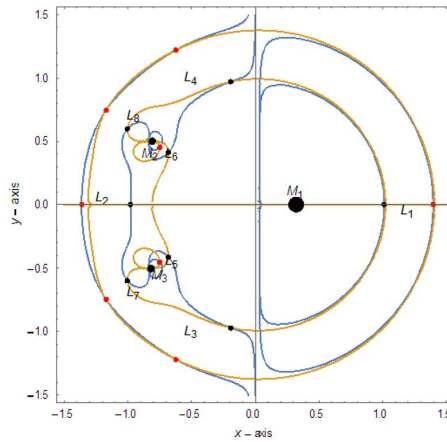


Figure 5. Concentric orbits under the Manev Potential and the Newton potential. The inner orbits with the black points is the Newtonian orbit while the outer orbit with the red points is the Manev orbit.

§4 Linear Stability

We study the linear stability of the motion of the test particle when a specific equilibrium point (x_0, y_0) experience small displacements τ and γ in the coordinates so that $x = x_0 + \tau$ and $y = y_0 + \gamma$. Consequently, the variational form of the equations of motion corresponding to Eqns.(2.1) are as given in (4.1)

$$\left. \begin{aligned} \ddot{\tau} - 2\alpha\dot{\gamma} &= \tau \left(\frac{\partial^2 \Omega}{\partial x^2} \right)_0 + \gamma \left(\frac{\partial^2 \Omega}{\partial x \partial y} \right)_0 \\ \ddot{\gamma} + 2\alpha\dot{\tau} &= \tau \left(\frac{\partial^2 \Omega}{\partial x \partial y} \right)_0 + \gamma \left(\frac{\partial^2 \Omega}{\partial y^2} \right)_0 \end{aligned} \right\} \quad (4.1)$$

Where the dots are the derivatives with respect to time t and the subscripts 0 implies the values are estimated at the equilibrium point (x_0, y_0) . Neglecting other higher terms in τ and γ , we took into cognizance only the linear terms in τ and γ . Supposing Eqns.(4.2) are the solutions of Eqns.(4.1)

$$\tau = \chi e^{\lambda t}, \quad \gamma = \Theta e^{\lambda t} \quad (4.2)$$

where χ, Θ are constants and λ is a parameter. Then the characteristic polynomial of the system (4.1) is derived as

$$\lambda^4 + a\lambda^2 + b = 0 \quad (4.3)$$

With

$$\begin{aligned} a &= 4\alpha^2 - \left(\frac{\partial^2 \Omega}{\partial x^2} \right)_0 - \left(\frac{\partial^2 \Omega}{\partial y^2} \right)_0 \\ b &= \left(\frac{\partial^2 \Omega}{\partial x^2} \right)_0 \left(\frac{\partial^2 \Omega}{\partial y^2} \right)_0 - \left(\frac{\partial^2 \Omega}{\partial x \partial y} \right)_0^2 \end{aligned}$$

$$\begin{aligned}
\left(\frac{\partial^2 \Omega}{\partial x^2}\right)_0 &= \beta + (1 - 2\mu) \left(-\frac{1}{r_{10}^3} + \frac{3(x_0 - \sqrt{3}\mu)^2}{r_{10}^5} \right. \\
&\quad \left. - \frac{3\sigma(1 - 2\mu)}{r_{10}^4} + \frac{12\sigma(1 - 2\mu)(x_0 - \sqrt{3}\mu)^2}{r_{10}^6} \right) \\
&\quad + \mu \left(-\frac{1}{r_{20}^3} + \frac{3(x_0 + \frac{1}{2}\sqrt{3}(1 - 2\mu))^2}{r_{20}^5} \right. \\
&\quad \left. - \frac{3\sigma\mu}{r_{20}^4} + \frac{12\sigma\mu(x_0 + \frac{1}{2}\sqrt{3}(1 - 2\mu))^2}{r_{20}^6} \right) \\
&\quad + \mu \left(-\frac{1}{r_{30}^3} + \frac{3(x_0 + \frac{1}{2}\sqrt{3}(1 - 2\mu))^2}{r_{30}^5} \right. \\
&\quad \left. - \frac{3\sigma\mu}{r_{30}^4} + \frac{12\sigma\mu(x_0 + \frac{1}{2}\sqrt{3}(1 - 2\mu))^2}{r_{30}^6} \right) \tag{4.4}
\end{aligned}$$

$$\begin{aligned}
\left(\frac{\partial^2 \Omega}{\partial y^2}\right)_0 &= \beta + (1 - 2\mu) \left(-\frac{1}{r_{10}^3} + \frac{3y_0^2}{r_{10}^5} - \frac{3\sigma(1 - 2\mu)}{r_{10}^4} + \frac{12\sigma(1 - 2\mu)y_0^2}{r_{10}^6} \right) \\
&\quad + \mu \left(-\frac{1}{r_{20}^3} + \frac{3(-\frac{1}{2} + y_0)^2}{r_{20}^5} - \frac{3\sigma\mu}{r_{20}^4} + \frac{12\sigma\mu(-\frac{1}{2} + y_0)^2}{r_{20}^6} \right) \\
&\quad + \mu \left(-\frac{1}{r_{30}^3} + \frac{3(\frac{1}{2} + y_0)^2}{r_{30}^5} - \frac{3\sigma\mu}{r_{30}^4} + \frac{12\sigma\mu(\frac{1}{2} + y_0)^2}{r_{30}^6} \right) \tag{4.5}
\end{aligned}$$

$$\begin{aligned}
\left(\frac{\partial^2 \Omega}{\partial x \partial y}\right)_0 &= (1 - 2\mu) \left(\frac{3y_0(x_0 - \sqrt{3}\mu)}{r_{10}^5} + \frac{12\sigma(1 - 2\mu)y_0(x_0 - \sqrt{3}\mu)}{r_{10}^6} \right) \\
&\quad + \mu \left(\frac{3(-\frac{1}{2} + y_0)(x_0 + \frac{1}{2}\sqrt{3}(1 - 2\mu))}{r_{20}^5} + \frac{12\sigma\mu(-\frac{1}{2} + y_0)(x_0 + \frac{1}{2}\sqrt{3}(1 - 2\mu))}{r_{20}^6} \right) \\
&\quad + \mu \left(\frac{3(\frac{1}{2} + y_0)(x_0 + \frac{1}{2}\sqrt{3}(1 - 2\mu))}{r_{30}^5} + \frac{12\sigma\mu(\frac{1}{2} + y_0)(x_0 + \frac{1}{2}\sqrt{3}(1 - 2\mu))}{r_{30}^6} \right) \tag{4.6}
\end{aligned}$$

with

$$\begin{aligned}
r_{10}^2 &= (x_0 - \sqrt{3}\mu)^2 + y_0^2 \\
r_{20}^2 &= (x_0 + \frac{1}{2}\sqrt{3}(1 - 2\mu))^2 + (y_0 - \frac{1}{2})^2 \\
r_{30}^2 &= (x_0 + \frac{1}{2}\sqrt{3}(1 - 2\mu))^2 + (y_0 + \frac{1}{2})^2 \\
r_0^2 &= x_0^2 + y_0^2
\end{aligned}$$

A libration point is considered to be linearly stable if Eqn (4.3) evaluated at that point has four complex roots all of which have negative real parts or all of which are purely imaginary, and this can only be if the under listed conditions are all satisfied

$$\begin{aligned} & \left(4\alpha^2 - \left(\frac{\partial^2\Omega}{\partial x^2}\right)_0 - \left(\frac{\partial^2\Omega}{\partial y^2}\right)_0\right)^2 - 4 \left(\left(\frac{\partial^2\Omega}{\partial x^2}\right)_0 \left(\frac{\partial^2\Omega}{\partial y^2}\right)_0 - \left(\frac{\partial^2\Omega}{\partial x\partial y}\right)_0^2\right) > 0 \\ & \left(4\alpha^2 - \left(\frac{\partial^2\Omega}{\partial x^2}\right)_0 - \left(\frac{\partial^2\Omega}{\partial y^2}\right)_0\right) > 0 \\ & \left(\left(\frac{\partial^2\Omega}{\partial x^2}\right)_0 \left(\frac{\partial^2\Omega}{\partial y^2}\right)_0 - \left(\frac{\partial^2\Omega}{\partial x\partial y}\right)_0^2\right) > 0 \end{aligned}$$

In the current study, the ancillary equation for the linear stability of the collinear libration points is

$$\lambda^4 + \left(4\alpha^2 - \left(\frac{\partial^2\Omega}{\partial x^2}\right)_0 - \left(\frac{\partial^2\Omega}{\partial y^2}\right)_0\right)\lambda^2 + \left(\frac{\partial^2\Omega}{\partial x^2}\right)_0 \left(\frac{\partial^2\Omega}{\partial y^2}\right)_0 = 0 \quad (4.7)$$

Since $\left(\frac{\partial^2\Omega}{\partial x\partial y}\right)_0 = 0$ at $y = 0$.

Table 3. Eigenvalues of the Libration points under Manev parameter ($\sigma = 0.8$).

	Equilibrium Points	$\lambda_{1,2}$	$\lambda_{3,4}$
L_1	(1.397620, 0)	0.858598 - 0.711316i	0.858598 + 0.711316i
L_2	(-1.36374, 0)	0.902262 - 0.773713i	0.902262 + 0.773713i
$L_{3,4}$	(-0.624035, 1.218980)	0.882602 - 0.752621i	0.882602 + 0.752621i
$L_{5,6}$	(-0.752644, 0.453444)	9.64689	6.28864i
$L_{7,8}$	(-1.170370, 0.747898)	0.800838 - 0.598697i	0.800838 + 0.598697i

Table 3 shows the computation of the eigen roots of (4.7) and (4.3) respectively for the libration points L_j , ($j=1,2,\dots,8$). It is observe that, under Manev potential, the motion of the test particle is unstable around all the libration points unlike in [14] where there were at least two stable equilibrium points in the case of Newtonian potential.

§5 Determination of Chaos by Lyapunov Characteristic Exponents

This tool has been used by researchers such as Kumari and Kushvah [21] to examine the presence of regularity or irregularity of the dynamical system. In application, if the orbits of the dynamical system divergence fast from each other, it implies difficulty to predict the behavior of the system, hence with regards to Dubeibe and Bermudez [22], any dynamical system which all of its Lyapunov exponents are not negative is chaotic. Using Mathematica package developed by Sandri [23], the first order LCEs of the system (2.1) is computed along with the graph in Fig (6). We have seen the presence of chaos in the system since the LCEs [1, 1,1, 1] are all positive exponents with respect to a set of arbitrary initial conditions [0.99977, 0.99977, 0.99977, 0.99977]. The LCEs observed here under Manev parameter ($\sigma = 0.8$.) differs from the one that whose equations of motion is governed by the Newtonian potential as shown in [15] where there is obvious divergence.

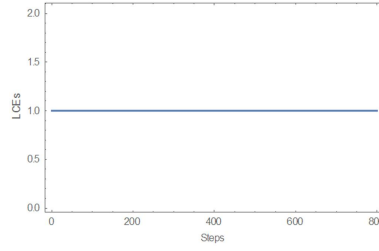


Figure 6. The Lyapunov Characteristic Exponents of the system.

§6 Numerical Applications of Model

We apply the model to astellar system, namely, 82 G. Eridani. This star is a high-velocity star—it is moving quickly compared to the average star and it is slightly smaller in size and less massive than the sun, making it marginally dimmer than the Sun in terms of luminosity. We compute the libration points for the motion of a grain in the vicinity of **82 G. Eridani**, **82 G. Eridani d**, and **82 G. Eridani e**. The mass of the primary star is $0.85 M_{sun}$. The other secondary stars **82 G. Eridani d**, and **82 G. Eridani e** both having equal mass $1.4414410^{-5} M_{sun}$. Thus, $\mu = 0.000016940602$. The libration points and the eigen roots for the stellar system are as shown in Tables (4) and (5) for the cases of Manev gravitational field and Newtonian gravitational field, respectively. In the Manev potential case, there exist nine equilibrium points for the stellar system, while there exist ten equilibrium points in the Newtonian case. In both cases, some of the equilibrium points are very close to each other as shown in figs 7 and 8 respectively. Fig (9) shows that the stellar system under Manev potential have a larger orbit, while the inner orbit represents the trajectories of the system under Newtonian potential. This proves that the motion of the system exhibits different behavior under different potentials. It is also found that all of the libration points for the stellar system are linearly unstable as tabulated in tables (4) and (5).

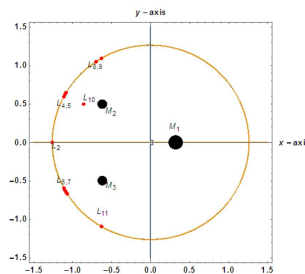


Figure 7. Libration points of **82 G. Eridani** Stellar System under Manev potential.

Table 4. Stability of libration points in the triple stellar system: **82 G. Eridani**, **82 G. Eridani d**, and **82 G. Eridani e** under Manev Potential ($\sigma = 0.8.$) and Centrifugal force ($\beta=1.4$).

	Equilibrium Points	$\lambda_{1,2}$	$\lambda_{3,4}$	Stability State
L_2	-1.26286, 0	1.15707	0.394102i	unstable
L_4	-1.08523, 0.645909	1.1586	0.397881i	Unstable
L_5	-1.10097, 0.618505	1.15947	0.399555i	Unstable
L_6	-1.10097, -0.618505	1.15947	0.399555i	Unstable
L_7	-1.08523, -0.645909	1.1586	0.397881i	Unstable
L_8	-0.701532, 1.05008	1.15724	0.394513i	Unstable
L_9	-0.631179, 1.09382	1.15722	0.394515i	Unstable
L_{10}	-0.863453, 0.498532	37.0683	26.1102i	Unstable
L_{11}	-0.631179, -1.09382	1.15722	0.394515i	Unstable

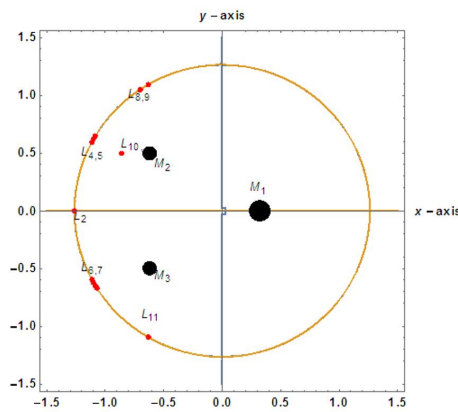


Figure 8. Libration points of **82 G. Eridani** Stellar System under Newtonian potential.

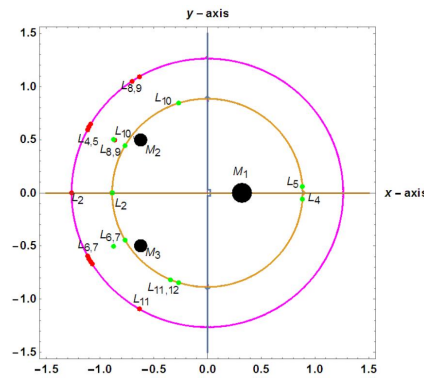


Figure 9. Equilibrium points of **82 G. Eridani** Stellar System under Manev potential (outer orbit with red points) versus Newtonian potential (inner orbit with green points).

Table 5. Stability of Libration points for the system: **82 G. Eridani, 82 G. Eridani d, and 82 G. Eridani e** under Newtonian Potential ($\sigma = 0$) and Centrifugal force ($\beta=1.4$).

	Equilibrium Points	$\lambda_{1,2}$	$\lambda_{3,4}$	Stability State
L_2	-0.885518, 0	0.740302	0.554813i	Unstable
L_4	0.883596, -0.0589214	0.742367	0.557724i	Unstable
L_5	0.883596, 0.0589214	0.742367	0.557724i	Unstable
L_6	-0.871247, -0.503032	12.3561	8.7692i	Unstable
L_7	-0.766466, 0.442894	0.786512	0.604951i	Unstable
L_8	-0.871247, -0.503032	12.3561	8.7692i	Unstable
L_9	-0.766466, -0.442894	0.786512	0.604951i	Unstable
L_{10}	-0.270192, 0.843309	0.741747	0.55692i	Unstable
L_{11}	-0.270192, -0.843309	0.741747	0.55692i	Unstable
L_{12}	-0.343067, -0.816376	0.742517	0.557876i	Unstable

§7 Discussion and Conclusion

We have carried out a numerical study on the existence, location, stability and dynamical behavior of the equilibrium points of an infinitesimal mass under small perturbations in the Coriolis and centrifugal forces in the restricted four-body problem when the primaries have Langrangian configuration with a generalized Manev potential. We have found eight equilibrium points, two of which are collinear and the remaining six non-collinear. The positions of the equilibrium points for the generalized Manev potential differ from the distribution of the equilibrium points when the Newtonian potential is only considered. We have also observed that the perturbations in the Coriolis and centrifugal forces caused the orbit of the infinitesimal body to shrink, which in the practical sense implies a decrease in the orbital elements. More so, due to the Manev potential, all of the equilibrium points are unstable in contrast to the Newtonian case where $L_{5,6}$ are stable (see, [14]). We found that an exploration model formulated on the Newtonian potential will assume a slightly different dynamical behavior and the orbital elements are lesser in values, for instance, the period of the motion than those of the model formulated by the Manev potential. More succinctly, we implemented the model to study the existence and stability of the equilibrium points of a stellar system 82 G. Eridani. In figures (7) and (8) show that the stellar system 82 G. Eridani under the Manev potential has nine equilibrium points which are distributed on the plane of motion in different pattern from the ten equilibrium points of the stellar system under the Newtonian potential. Furthermore, as shown in figure (9), taking the stellar system 82 G. Eridani as a case study and supposing the primaries are luminous, the electro-mechanical components of a space asset on the Newtonian orbit might suffer higher adverse effect than a space asset on a Manev orbit since the Newtonian (inner) orbit is closer to the primaries. These findings show clearly that a few-body model derived on the basis of the usual Newtonian potential is an approximation to that of the generalized Manev potential. Consequently, there is a need for onward researches that consider

the Manev potential instead of the classical Newtonian potential, since there are ample dynamical possibilities for varieties of results and newer innovative applications in astronomy, space sciences and technology. The LCEs of the system was computed using a Mathematica package and we found that it is a chaotic system because all of the exponents are non-negative.

References

- [1] I Newton. *The Principia: Mathematical Principles of Natural Philosophy*, University of California Press, 1999.
- [2] F N Diacu. *Near collision dynamics for particle systems with quasihomogeneous potentials*, J Differential Equations, 1996, 128(1): 58-77.
- [3] G Maneff. *La gravitation et le principe de l'egalie de l'action et de la reaction*, C R Acad Sci Paris, 1924, 178: 2159-2161.
- [4] K Popoff. *Die Gravitation und das Prinzip von Wirkung und Gegenwirkung*, Z f Phys, 1925, 32: 7403-405.
- [5] G Maneff. *Die Masse der Feldenergie und die Gravitation*, Astron Nach, 1929, 236: 401-406.
- [6] G Maneff. *La gravitation et l'energie au zero*, C R Acad Sci Paris, 1930, 190: 1374-1377.
- [7] C Blaga. *Prescencing orbits, central forces and Manev potential*, In: V Gerdjikov and M Tsetkov, Eds, Prof. G Manevs Legacy in Contemporary Astronomy, Theoretical and Gravitational Physics, Heron Press, Chicago, 2015, 134-139
- [8] R Ivanov, E Prodanov. *Manev Potential and general relativity*, Prof. G Manev's Legacy in Contemporary Astronomy, Theoretical and Gravitational Physics, Heron Press, Sofia, 2005, DOI: 10.21427/saqqf53.
- [9] I Haranas, V Mioc. *Manev Potential and Satellite orbits*, Rom. Astron J, 2009, 19: 153-166.
- [10] S Kirk, I Haranas, I Gkigkitzis. *Satellite motion in a Manev Potential with drag*, Astrophysics Space Sci, 2013, 344: 313-320.
- [11] C Blaga. *Stability in sense of Lyapunov of Circular orbits in Manev Potential*, Romanian Astron J, 2015, 25: 233-240.
- [12] E Barrabés, J M Cors, C Vidal. *Spatial collinear restricted four body problem with repulsive mane v potential*, Celestial Mech Dynam Astronom, 2017, 129: 153-176.
- [13] K P Bhatnager, P P Hallan. *Effect of perturbations in Coriolis and centrifugal forces on the stability of liberation points in the restricted problem*, Celest Mech, 1978, 18: 105-112.
- [14] J Singh, V E Aguda. *Effect of perturbations in the Coriolis and centrifugal Forces on the Stability of Equilibrium Points in the Restricted Four-Body Problem*, Few-Body Syst, 2015, 56(10): 713-723.
- [15] J Singh, S O Omale. *Combined Effect of Stokes Drag, Oblateness and Radiation Pressure on the Existence and Stability of Equilibrium Points in the Restricted Four-Body Problem*, Astrophys Space Sci, 2019, 364 (6), <https://doi.org/10.1007/s10509-019-3494-3>.

- [16] J Singh, S O Omale. *A study on bi-circular R4BP with dissipative forces: Motion of a spacecraft in the earth-moon-focused view*, Few-Body Systems, 2020, 61(2): 1-14.
- [17] A E Vincent, J J Taura, S O Omale. *Existence and stability of equilibrium points in the photogravitational restricted four-body problem with Stokes drag effect*, Astrophysics and Space Science, 2019, 364 (10): 1-13.
- [18] I A Abouelmagad, H M Asiri, M A Sharaf. *The effect of oblateness in the perturbed restricted three-body problem*, Meccanica, 2013, 48: 2479-2490.
- [19] F L Dubeibe, F D Lora-Clavijo, A G Guillermo. *Pseudo-Newtonian planar circular restricted 3-body problem*, Physics Letters A, 2016, 381(6): 563.
- [20] A N Baltagiannis, K E Papadakis. *Equilibrium points and their stability in the restricted four-body problem*, Int J Bifurcat Chaos Appl Sci Eng, 2011, 21: 2179-2193.
- [21] R Kumari, B S Kushvah. *Equilibrium points and zero velocity surfaces in the restricted four-body problem with solar wind drag*, Astrophys Space Sci, 2013, 344: 347-359.
- [22] F L Dubeibe, L D Bermúdez-Almanza. *Optimal conditions for the numerical calculation of the largest lyapunov exponent for systems of ordinary differential equations*, Int Journal of Modern Physics C, 2014, 25(7): 1450024.
- [23] M Sandri. *Numerical calculation of Lyapunov Exponents*, University of Verona, Italy, The Mathematica Journal, Miller Freeman Publications, 1996.

¹Department of Mathematics, Faculty of Physical Sciences, Ahmadu Bello University, Zaria, Nigeria.
Email: jgds2004@yahoo.com

²Department of Engineering and Space Systems, National Space Research and Development Agency (NASRDA), Obasanjo Space Centre, Abuja, Nigeria.
Email: solomondavidson1203@gmail.com